

# Pulse Phase Spectroscopy of A 0535+26 during its 1994 giant outburst observed with OSSE

Michael Maisack<sup>1</sup>, J. Eric Grove<sup>2</sup>, Eckhard Kendziorra<sup>1</sup>, Peter Kretschmar<sup>1</sup>, Rüdiger Staubert<sup>1</sup>, and Mark S. Strickman<sup>2</sup>

<sup>1</sup> Institut für Astronomie und Astrophysik, Abteilung Astronomie, Universität Tübingen, 72076 Tübingen, Germany

<sup>2</sup> E.O. Hulburt Center for Space Research, Naval Research Laboratory, Washington, DC 20375, USA

Received 1997; accepted XXX

**Abstract.** We present pulse phase spectroscopy of A 0535+26 in the energy range 35-200 keV from OSSE observations of its giant outburst in 1994. We discuss the phase dependence of the continuum parameters and the cyclotron resonance feature (CRF) at 110 keV already found in the phase averaged spectrum. We find that a CRF is required at every phase. The behaviour of the line parameters with phase and the pulse shape indicate that the emission occurs in a pencil-beam geometry.

**Key words:** Stars: magnetic fields; Stars: neutron; Gamma rays: observations

## 1. Introduction

In Be X-ray binaries (BeXRB) with a neutron star as the compact object, mass transfer is mediated via a circumstellar disk around the companion. The companions are O or B stars with high rotational velocities which are responsible for the loss of material in the equatorial plane. The material in this disk, which may be present or absent for extended periods, flows out rather slowly (velocities of several tens of km/s) compared to the fast B star wind outside the equatorial plane. In fact, the dynamics of the material in this circumstellar disk may be dominated by Keplerian motion (e.g. Hanuschik 1996).

BeXRB undergo dramatic increases in X-ray flux when the neutron star passes through the dense regions of the circumstellar disk near periastron passage and enhanced mass accretion sets in. Outbursts with luminosities in excess of  $10^{38}$  ergs/s can be observed in these systems at these times, while the X-ray luminosity during quiescence is  $10^{33}$  ergs/s and below.

*Send offprint requests to:* M. Maisack, maisack@astro.uni-tuebingen.de

The brightest object of this class is the system A 0535+26 (HDE 245770), which has an orbital period of  $\approx 110$  days, and a pulsation period of  $\approx 103$  s. For a comprehensive review of the system properties, see Giovannelli and Graziati (1992). The system shows relatively regular outbursts occurring near periastron passage, and occasional giant outbursts during which the system becomes several times brighter than the Crab between  $\approx 5$  and 100 keV. The system has also been found in prolonged off states (Motch et al. 1991).

Four giant outbursts have been observed so far; during the last two of these in 1989 and 1994, cyclotron lines (also called cyclotron resonance features, CRF) have been observed (Kendziorra et al. 1994, Grove et al. 1995). CRF in the X-ray regime are produced in very high magnetic fields ( $B > 10^{11-12}$  G), where the cyclotron energy becomes comparable to the electron rest mass. The electrons can then only gyrate on discrete Landau levels. Transitions between these levels result in line features in the X-ray spectra.

Kendziorra et al. (1994) found two features in the phase resolved TTM/HEXE spectra of A 0535+26 at  $\approx 50$  and 100 keV, whereas Grove et al. (1995) found a feature only at  $\approx 110$  keV in the phase averaged spectrum during an outburst observed by OSSE. However, the presence of a feature at  $\approx 50$  keV could not be ruled out due to the higher energy threshold of OSSE compared to TTM/HEXE. Regardless of the existence of the 50 keV feature, the magnetic field of the neutron star in A 0535+26 is the highest that has been measured directly so far (for a review of cyclotron line sources, see Makishima and Mihara 1992).

In this paper, we present pulse phase resolved spectroscopy of the 1994 outburst observed by OSSE. We discuss the variability of the continuum and the 110 keV line feature across the pulse, the possibility of the presence of a feature at  $\approx 50$  keV and physical implications for the emission pattern at the magnetic poles.

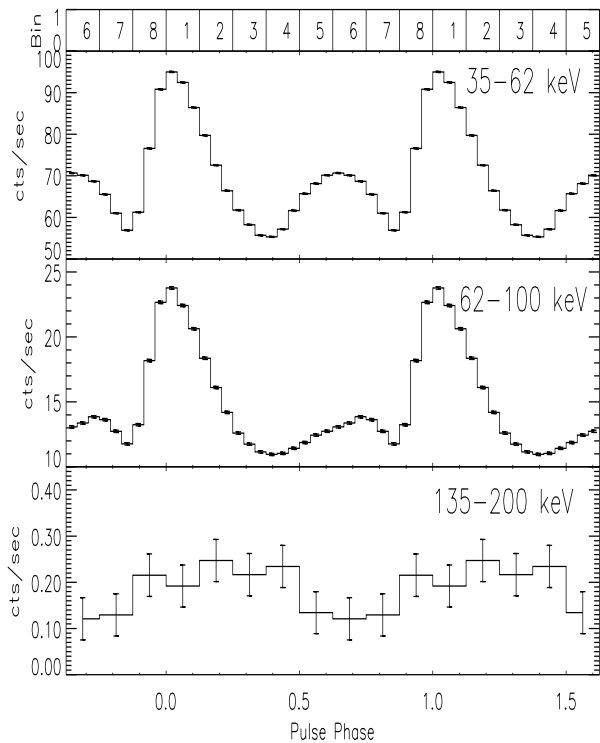


**Fig. 1.** Background-subtracted pulse profiles of A 0535+26 in the energy ranges 35-62, 62-100 and 135-200 keV. The former two have 24 phase bins, the latter has been rebinned to 8 phase bins. Note suppressed zero in upper two panels. Numbering of phase bins is displayed on top.

## 2. Observations and Data Analysis

OSSE is one of the 4 instruments on CGRO. It is a phoswich-type collimated scintillation counter sensitive between 35 keV and 10 MeV. It consists of four identical detectors which are collimated to a field of view of  $3.8 \times 11.4$  degrees (FWHM). The total effective area at 511 keV is  $2000 \text{ cm}^2$ . The energy resolution is 23% (FWHM) at 50 keV and 15% at 100 keV. Observations are performed by rocking the four detector modules between source and source-free background fields on either side of the source field along the scan axis in a predefined sequence. A detailed description of the instrument and the data analysis techniques is given in Johnson et al. (1993). Following Grove et al. (1995), we include a 3% systematic error in spectral measurements.

The onset of a giant outburst of A 0535+26 was detected by BATSE in January 1994 (Finger et al. 1994). An observation with OSSE was performed from 1994 Feb 8-17. Phase averaged spectral analysis with the detection of the cyclotron line has been presented by Grove et al. (1995). The pulse profiles in the OSSE energy range have

already been discussed by Maisack et al. (1996): the profile has two peaks, the so-called "main pulse" centered on phase 0 is more prominent and has a harder spectrum, whereas the secondary pulse at phase 0.6 has a softer spectrum (see also Kretschmar et al. 1996). The pulse profiles in the energy ranges 35-62, 62-100 and 135-200 keV are shown in Fig.1. The shape of the profile is similar in all three energy bands.

## 3. Spectral fits

For our phase resolved spectral fits, we use 8 phase bins (corresponding to  $\approx 13 \text{ sec/bin}$ ). This number was chosen to ensure that there is a statistically significant signal above 100 keV in each phase bin. For the spectral fits, we use the same model as Grove et al. (1995) for the phase averaged spectrum, given by Tanaka (1986), in which the continuum is described by an exponentially truncated power law modified by two Lorentzian absorption lines:

$$N(E) = I_{70 \text{ keV}} (E/70)^{-\alpha} \exp(-E/E_F) \exp(-B) \quad (1)$$

where

$$B = \tau_1 \frac{W^2 (E/E_C)^2}{(E - E_C)^2 + W^2} + \tau_2 \frac{(2W)^2 (E/2E_C)^2}{(E - 2E_C)^2 + (2W)^2} \quad (2)$$

Here,  $I_{70 \text{ keV}}$  is the continuum normalisation at 70 keV,  $\alpha$  is the photon index and  $E_F$  is the e-folding energy of the continuum,  $E_C$  the line centroid energy,  $W$  and  $2 \times W$  the half widths (HWHM) and  $\tau_n$  the optical depths of the individual cyclotron lines. The energies are given in keV. The choice of Lorentzian lines is motivated by the need for an analytic formula. While the profiles are expected to have more complicated shapes (e.g. Araya and Harding 1996), the energy resolution of OSSE at 100 keV is 15%, crude enough to justify the use of such a simple approach.

Analysis of the pulse shape and hardness ratios has shown that the spectrum varies with phase (Maisack et al. 1996). To verify this in our detailed phase resolved spectral analysis, we first attempted to fit the best-fit continuum of the phase averaged spectrum from Grove et al. (1995) with the normalisation as the only free parameter to each individual phase spectrum. This yields unacceptable fits (probability  $< 1\%$ ) for most phase bins, confirming that the spectrum changes with phase.

Next, we tried to fit a simple continuum without line structures to the individual phase spectra, i.e. the only free parameters in this model are the normalisation, power law index and e-folding energy. This model yields marginally acceptable fits (probability  $< 10\%$ ) only for the two phase bins with the lowest intensity. If the power law index is fixed at the TMM/HEXE value of 1.2 (see below for an extended justification of this choice), no acceptable fits are achieved. This is convincing evidence that additional spectral features are present at every phase.

Phase Bin	$\chi_\nu$	$I_{70keV}$	$E_F[keV]$	$E_C[keV]$	$\tau_2$
1	0.80	$3.69 \pm 0.07$	$28.5 \pm 0.8$	$114.9 \pm 0.7$	$2.55 \pm 0.11$
2	0.75	$3.42 \pm 0.06$	$27.2 \pm 0.7$	$115.6 \pm 0.7$	$2.31 \pm 0.10$
3	0.72	$2.30 \pm 0.04$	$23.5 \pm 0.6$	$116.8 \pm 1.3$	$1.78 \pm 0.11$
4	0.92	$1.94 \pm 0.05$	$23.3 \pm 0.8$	$111.6 \pm 1.3$	$1.66 \pm 0.12$
5	0.55	$2.05 \pm 0.05$	$22.8 \pm 0.6$	$109.9 \pm 1.0$	$1.74 \pm 0.09$
6	0.68	$2.24 \pm 0.06$	$22.6 \pm 0.6$	$107.8 \pm 0.9$	$1.63 \pm 0.10$
7	0.69	$2.34 \pm 0.05$	$23.6 \pm 0.7$	$110.8 \pm 0.9$	$1.85 \pm 0.10$
8	0.95	$2.62 \pm 0.06$	$25.5 \pm 0.8$	$115.2 \pm 1.2$	$2.37 \pm 0.15$

**Table 1.** Best fit parameters for the phase resolved data in 8 phase bins.  $I_{70keV}$  is the continuum intensity at 70 keV in  $10^{-3}$  photons  $(\text{cm}^2 \text{ s keV})^{-1}$ ,  $E_F$  the e-folding energy in keV,  $E_C$  the line centroid energy in keV and  $\tau_2$  the depth of the line.

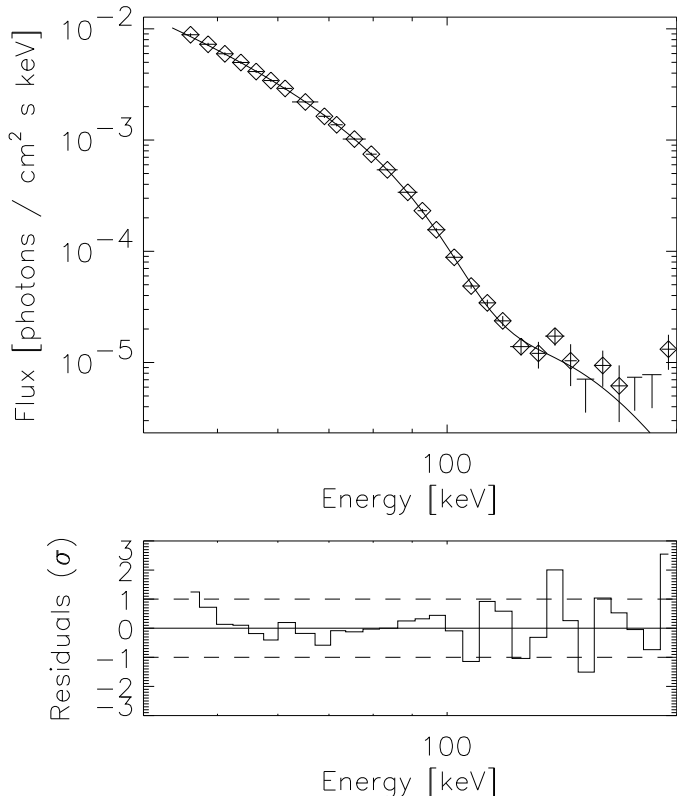


**Fig. 2.** Best fit photon spectrum and fit residuals for phase bin 1

Next, we tried to leave all parameters free for each phase spectrum, i.e. to allow for two line features. The model yields acceptable fits for all phase spectra; however, the statistical quality of individual phase spectra is not sufficient to derive meaningful constraints on the parameters. As in the phase averaged spectrum, the depth of the first line is consistent with zero, i.e. the 50 keV feature seen by HEXE (Kendziorra et al. 1994) is not required at any phase by the OSSE data, but serves only to flatten the continuum at low energies. In these fits with all parameters free, the continuum parameters in particular (i.e. power law index and e-folding energy) cannot be constrained

since the OSSE energy range  $> 35$  keV provides no good handle on the power law part of the spectrum. Since both phase averaged and phase resolved TTM/HEXE spectra (Kretschmar et al. 1996) are consistent with  $\alpha=1.2$ , with no evidence for variability with phase and overall intensity, we adopt this value as a fixed parameter for the OSSE spectral fits. This means that the e-folding energy carries the information about the hardness of the continuum. Moreover, the energy resolution of the OSSE instrument (see Johnson et al. 1993) is not sufficient to independently constrain the depth and HWHM of the line. We therefore keep the HWHM of the line at  $\approx 50$  keV fixed at 15 keV (this value is the average HWHM from fits of all phase bins, and consistent with the spectrum of each individual phase bin) and leave the line centroid energy and the depth as the free parameters. Note that the HWHM of the line at  $\approx 110$  keV is then 30 keV.

We therefore fit all individual spectra with line width and power law index fixed, and the e-folding energy, line centroid, line depth and continuum normalisation free. This yields acceptable fits for all phase spectra. Again, a CRF at  $\approx 50$  keV is possible, but not required, and the  $2\sigma$  upper limit for the depth is  $\tau_1=0.15$ .

Since all phase bin fits are consistent with no CRF at 50 keV, we keep the depth of the 50 keV feature fixed at zero and only fit a CRF at  $\approx 110$  keV (with HWHM 30 keV). We find that such a CRF is then required at every phase, and that the line centroid energy and line depth vary. The fit results and parameters are listed in Table 1 and displayed in Fig.3. As an example, the unfolded spectrum and fit residuals for bin 1 are shown in Fig. 2.

#### 4. Variation of parameters with phase

In this section, we discuss the dependence of the individual fit parameters on phase for the fits with a CRF at  $\approx 110$  keV, the photon index and line width fixed and no CRF at  $\approx 50$  keV. We find that the continuum is hardest during the main pulse, with an e-folding energy of up to 28 keV, while the secondary pulse and interpulse phases only have an e-folding energy of  $\approx 23$  keV. This parameter traces the continuum intensity at 70 keV well. The line centroid energy is also found to vary with phase. During

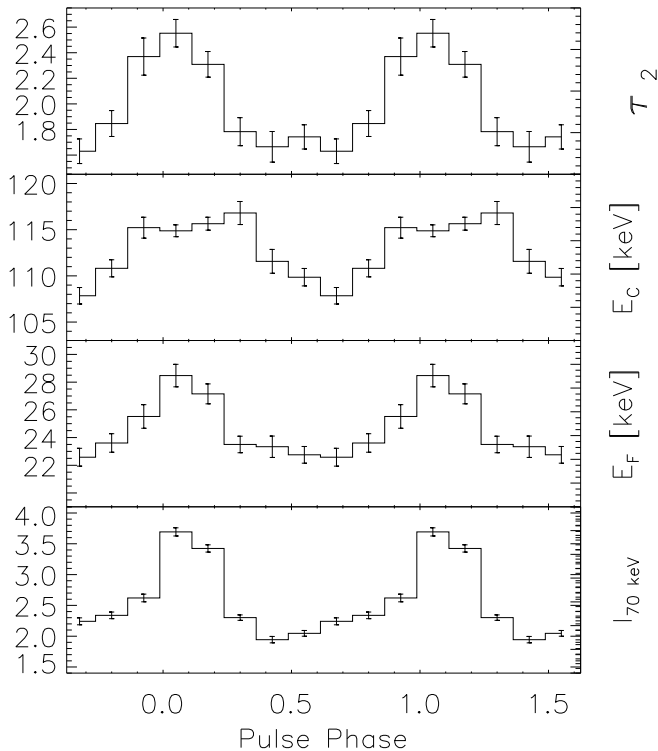


**Fig. 3.** Dependence of fit parameters on phase.

the main pulse, the centroid energy is 116 keV, compared to 109 keV during the secondary pulse.

From Fig.3, it can be seen that continuum intensity  $I_{70 \text{ keV}}$ , the e-folding energy  $E_F$  and the line depth  $\tau_2$  have essentially identical phase dependence. The line centroid energy,  $E_C$ , also varies with phase, being highest during the main peak, however, the behaviour of this parameter with phase does not exactly trace that of the other parameters. The line centroid energy is already at its high level of 116 keV before the onset of the main pulse, and remains at that level for about half the period. Using 16 phase bins to achieve better temporal resolution across the phase, one finds that the increase in the line centroid energy is indeed rather abrupt, with a more gradual decline after the main pulse.

#### 4.1. Variability during the observation

As has already been shown for the phase averaged spectrum by Maisack et al. (1996), the spectrum becomes softer as the intensity increases during the 10 days of the OSSE observation. To show that this is the case for every individual phase bin, we divide the observation into two halves of 5 days each (Feb 8-12 and Feb 13-17). As can be seen from Fig. 4, the e-folding energy is lower (i.e.

the spectrum is steeper) in the later, brighter half of the observation.

It is a useful exercise to check the variations of the line centroid energy between the early and late halves of the observation. Changes in that parameter cannot be due to a sudden change in the neutron star’s magnetic field and instead convey the systematic uncertainties introduced by the varying continuum spectra. The differences between the best fit line centroid energies are shown in Fig. 5 in the same fashion as those for the e-folding energy in the previous figure. One can see that the phase-dependent trends persist, and that the absolute value of the centroid energy is subject to a systematic uncertainty of less than 2 keV depending on the steepness of the continuum.

## 5. Discussion

As in the phase averaged analysis, we find a cyclotron feature at  $\approx 110$  keV in each of the 8 phase bins used for this analysis, whereas a line at half this energy is possible but never required. Nagel (1981) predicts that the pulse profile changes from double peaked below the cyclotron energy to single peaked above for pencil beam configuration at moderate optical depth (for which we will argue below). As there is no sign of a change in beam pattern at the putative line energy of  $\approx 50$  keV, we conclude that the feature at 110 keV is the fundamental line. The OSSE data above 110 keV, i.e. in the energy range 135-200 keV (see Fig. 1), however, are not statistically significant enough to determine the possible presence of the secondary peak.

The interdependence of the individual spectral parameters can be used to obtain information about the emission mechanisms and emission patterns of A 0535+26. We find that the line centroid energy is positively correlated with the intensity. This is generally expected from a pencil beam emission pattern (e.g. Nagel 1981, Meszaros and Nagel 1985). Supporting evidence for this comes from the positive correlation between continuum intensity and spectral hardness, which is also an indication of a pencil beam (Nagel 1981). Additional constraints can be derived from the line parameters: as photons propagating parallel to the field lines are most easily scattered, the line deficit is expected to be highest as one views directly onto the magnetic poles. As this line deficit (parameterised by the line depth) varies in phase with the line centroid energy, this is yet another indicator for the pencil beam pattern.

The line centroid energy is highest when the emission region is viewed parallel to the magnetic field, and is expected to vary with angle  $\theta$  (Harding and Daugherty 1991) as

$$h\nu = \frac{m_e c^2}{\sin^2 \theta} (\sqrt{1 + 2nB \sin^2 \theta} - 1) \quad (3)$$

For a line at  $\approx 110$  keV, the expected variation with angle is thus 10 keV, approximately the range that is ob-

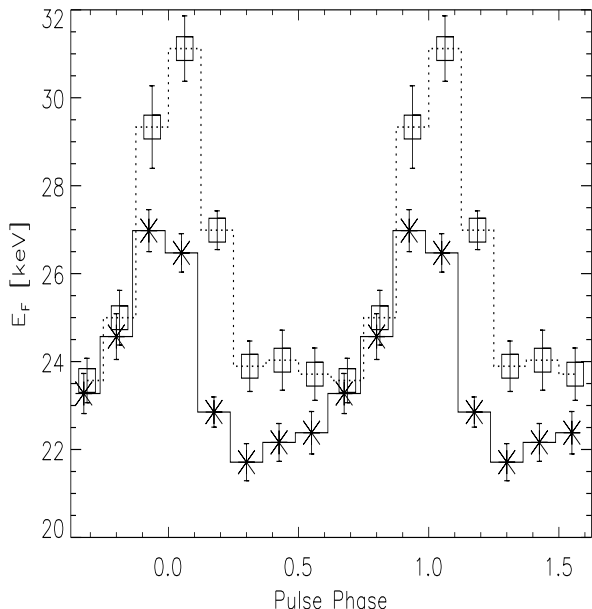


**Fig. 4.** Comparison of best fit e-folding energies for early (squares) and late (asterisks) parts of the observation.

served. The width of the line is expected to vary due to thermal Doppler broadening (Harding 1994) as

$$\Delta\omega = \omega\sqrt{(2kT/m_e c^2)\cos(\theta)} \quad (4)$$

where  $kT$  is the electron temperature. An electron temperature of  $\approx 7$ -10 keV can be estimated from the cutoff in the X-ray spectrum, which occurs between 20 and 30 keV (Kretschmar et al. 1996). According to the above equation, the line at  $\theta=0$  would then be broadened by 20 keV. Since the HWHM of the 110 keV line is fixed at 30 keV, this is consistent with our observations.

A full account of the effects of gravitational light bending is also required to fully model the emission pattern (e.g. Meszaros and Riffert 1988, Riffert and Meszaros 1988) and to determine whether the second peak is due to emission from the other pole or not. Modelling of these effects has been performed by Kraus et al. (1995) for Cen X-3. However, unique solutions of this model can only be derived if there exist profiles at different energies that display significantly different pulse shapes. The profiles obtained between 35 and 200 keV in this observation are too similar for this type of analysis, but future observations by SAX or XTE could be used to address this issue.

Our finding that the emission pattern is most likely a pencil beam is surprising in view of the high luminosity of A 0535+26 during the outburst, which exceeds  $10^{36}$  ergs/s even above 45 keV (Grove et al. 1995). For X-ray luminosities in excess of several  $10^{36}$  ergs/s, one generally expects a radiative shock which is optically thick in the field direction, resulting in a fan beam emission pattern from an

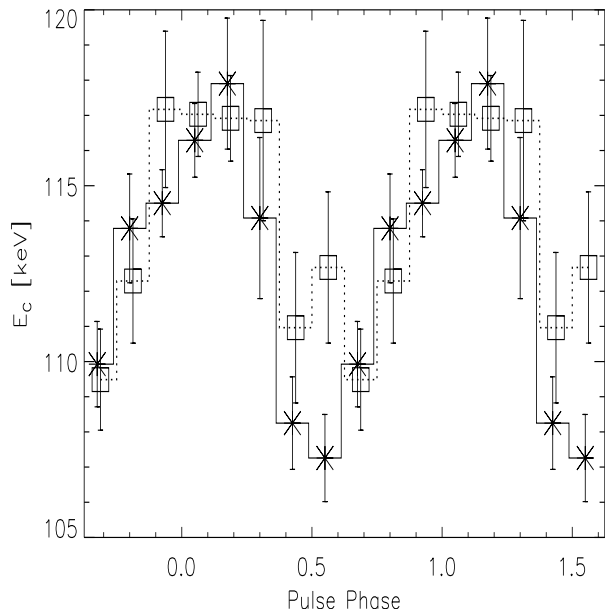


**Fig. 5.** Comparison of best fit line centroid energies for early (squares) and late (asterisks) parts of the observation.

accretion cylinder (also called accretion column), whereas for lower luminosities a collisionless shock results in an optically thin slab which emits a pencil beam pattern (e.g. Basko and Sunyaev 1976). We point out that contrary to these expectations, Her X-1 also shows these signatures of pencil beam emission (e.g. Harding 1994). The high optical depth parallel to the field lines expected for the high luminosity case could be circumvented by *photon bubbles*, which can rise and escape from the polar cap through the accretion column (Klein et al. 1996a). Such bubbles have been used to explain QPO seen in GRO J1744-28 and Sco X-1 (Klein et al. 1996b). We point out that similar QPO have been detected from A 0535+26 by BATSE during the 1994 giant outburst (Finger et al. 1996).

### 5.1. About the possible 50 keV feature

The CRF at  $\approx 50$  keV which was found in the TTM/HEXE data – albeit at low significance – of the 1989 giant outburst is not required by the OSSE data, but serves to flatten the continuum at low energies. The lack of a change of the pulse profile from double to single peaked above this energy (Nagel 1981) argues against a CRF at this energy (under the assumption of a pencil beam emission pattern). Analysis of the line shape in the OSSE data by Araya and Harding (1996) also provided evidence that the CRF at 110 keV is the fundamental line. Since  $kT \ll h\omega_B$ , most electrons will populate the ground Landau state (Harding 1994), and the fundamental line should be substantially deeper than a harmonic.

This would require that a possible fundamental at 50 keV would have to be favourably filled by photons generated by photon spawning, or hidden by a complicated geometry (Araya and Harding 1996).

## 6. Conclusions

We have studied the phase resolved spectrum of A 0535+26 during a giant outburst. While energy dependent pulse shapes and phase resolved spectra do not support the presence of a CRF at  $\approx 50$  keV, it cannot be completely ruled out, so this issue needs to be addressed by instruments with better low energy coverage, e.g. SAX or XTE. We observe the feature at 110 keV at each of the 8 phase bins used. The interdependence of individual model parameters indicate a pencil beam emission pattern, contrary to expectations from high luminosity sources. Also taking into account gravitational redshifts, we expect the magnetic field of A 0535+26 to be in excess of  $10^{13}$  G.

This observation was possible due to the outstanding brightness of A 0535+26 during a giant outburst. Taking into account the steepness of X-ray binary pulsar spectra at high energies, detections of even higher energy CRFs will be a difficult task even for future instruments with a sensitivity which is expected to be a factor of 10 better than achieved in this observation.

*Acknowledgements.* This work was supported under DARA grant 50 OR 92054 and NASA contract S-10987-C.

## References

- Araya, R. and Harding, A.K. 1996. ApJ 463, L33  
 Basko, M.M. and Sunyaev, R.A. 1976. MNRAS 175, 395  
 Finger, M.H., Wilson, R.B. and Hagedorn, K.S. 1994. IAUC 5931  
 Finger, M.H., Wilson, R.B. and Harmon, B.A. 1996. ApJ 459, 288  
 Giovannelli, F. and Graziati, L.S. 1992. SSR, 59, 1  
 Grove, J.E., Strickman, M.S., Johnson, W.N. et al. 1995. ApJ 438, L25  
 Harding, A.K. and Daugherty, J.K. 1991. ApJ 374, 687  
 Harding, A.K. 1994. AIP 308 (2nd Compton Symposium), 429  
 Hanuschik, R. 1996. A&A 308, 170  
 Johnson, W.N., Kinzer, R.L., Kurfess, J.D. et al. 1993. ApJS 86, 693  
 Kendziorra, E., Kretschmar, P., Pan, H.C. et al. 1994. A&A 291, L31  
 Klein, R.I., Arons, J., Jernigan, J.G. et al. 1996a. ApJ 457, L85  
 Klein, R.I., Jernigan, J.G., Arons, J. et al. 1996b. ApJ 469, L119  
 Kraus, U., Blum, S., Schulte, J. et al. 1996. ApJ 467, 794  
 Kretschmar, P., Pan, H.C., Kendziorra, E. et al. 1996. A&AS, Vol 120., No.4, 175  
 Maisack, M., Grove, J.E., Johnson, W.N. et al. 1996. A&AS, Vol. 120, No. 4, 179  
 Makishima, K. and Mihara, T. 1992. in: *Frontiers of X-Ray Astronomy*, Universal Academy Press, p.23

- Meszaros, P. and Nagel, W. 1985. ApJ 299, 138  
 Meszaros, P. and Riffert, H. 1988. ApJ 327, 712  
 Motch, C., Stella, L., Janot-Pacheco, E. et al. 1991. ApJ 369, 490  
 Nagel, W. 1981. ApJ 251, 278  
 Riffert, H. and Meszaros, P. 1988. ApJ 325, 207  
 Tanaka, Y. 1986. in: *Radiation Hydrodynamics in Stars and Compact Objects*, eds. D. Mihalas and K. Winkler (Berlin: Springer), 198